C. R. Geoscience 342 (2010) 676–684

Contents lists available at ScienceDirect

Comptes Rendus Geoscience

www.sciencedirect.com

Geomaterials (Mineralogy)

The dependence of albite feldspar dissolution kinetics on fluid saturation state at acid and basic pH: Progress towards a universal relation

Cinétique de dissolution de l'albite en fonction du degré de saturation du fluide à pH acide et basique : vers une relation universelle

Roland Hellmann [a,*], Damien Daval [b,c], Delphine Tisserand [a]

[a] *Environmental Geochemistry, LGIT, CNRS UMR C5559, University of Grenoble I, OSUG, BP 53X, 38041 Grenoble cedex 9, France*
[b] *CNRS UMR 8538, laboratoire de géologie, École normale supérieure de Paris, 24, rue Lhomond, 75231 Paris cedex 05, France*
[c] *Institut de physique du globe de Paris, centre de recherches sur le stockage géologique du CO_2, 4, place Jussieu, 75005 Paris, France*

ARTICLE INFO

Article history:
Received 3 November 2008
Accepted after revision 2 June 2009
Available online 7 August 2009

Written on invitation of the Editorial Board

Keywords:
Feldspar
Albite
Dissolution
Kinetic rate laws
Gibbs free energy
Water–rock interaction
CO_2 sequestration

Mots clés :
Feldspath
Albite
Dissolution
Lois cinétiques
Enthalpie libre
Interactions fluide–roche
Séquestration du CO_2

ABSTRACT

Here we report on two separate ongoing, multi-year investigations on the dependence of the dissolution rate (R) of albite feldspar on fluid saturation state, as defined by the Gibbs free energy of reaction (ΔG_r) for dissolution. The investigations are based on dissolution at pH 9.2, 150 °C and pH 3.3, 100 °C. Both studies reveal that the R–ΔG_r relation is highly non-linear and sigmoidal. The kinetic data from the first study, being the most complete, can be fitted with a sigmoidal rate curve that is composed of two separate, parallel rate laws that represent distinct mechanisms of dissolution. The switch between one dominant mechanism and the other may be controlled by a critical free energy. The fact that in both studies the same type of sigmoidal R–ΔG_r relation exists for dissolution at different pH and temperature condition suggests that this behavior may be universal for albite and other feldspars. Moreover, the experimental data contradict the commonly used R–ΔG_r relation that is loosely based on transition state theory (TST). This has important implications with respect to the accuracy of geochemical codes that model water–rock interactions at near-equilibrium conditions.

RÉSUMÉ

Cette étude compare les résultats de deux séries d'expériences en cours sur la cinétique de dissolution de l'albite (R), en fonction de l'enthalpie libre de cette réaction (ΔG_r). La première a été conduite à 150 °C et à un pH de 9,2, la seconde à 100 °C et à un pH de 3,3. Chacune des deux études révèle que la relation entre R et ΔG_r est sigmoïdale. Le jeu de données de la première série d'expériences peut être reproduit à l'aide d'une courbe paramétrée. La formulation de cette courbe repose sur deux lois cinétiques parallèles, décrivant deux mécanismes de dissolution distincts. Le basculement d'un mécanisme prédominant par rapport à l'autre est probablement contrôlé par une valeur critique de ΔG_r. L'existence d'une relation sigmoïdale unique en dépit des différences de conditions expérimentales suggère que ce comportement est caractéristique et universel pour l'albite et probablement plus généralement pour les feldspaths. De plus, les données expérimentales sont en contradiction avec la formulation classique des relations R–ΔG_r basée sur la théorie de l'état de transition (TST), qui est implémentée dans la plupart des

* Corresponding author.
E-mail address: roland.hellmann@obs.ujf-grenoble.fr (R. Hellmann).

1631-0713/$ – see front matter © 2009 Académie des sciences. Published by Elsevier Masson SAS. All rights reserved.
doi:10.1016/j.crte.2009.06.004

codes géochimiques. Elle serait donc une source importante d'imprécision proche des conditions d'équilibre chimique lors des simulations numériques.

1. Introduction

Fluid–solid interactions play a key role in many fields, in particular chemistry, materials science, ecology and biology, and the Earth sciences. The rate of decomposition or dissolution of a solid in contact with a fluid is a parameter of fundamental importance, and depends on the specific properties of both the solid and fluid. In the Earth sciences, of primordial concern are rates of water–rock interactions that occur at the surface and near surface within the upper crust. In order to fully understand the kinetics of chemical weathering associated with water–rock interactions, it has long been recognized that this requires determining the rate at which the individual components of rocks, i.e. single minerals, react in the presence of aqueous fluids.

Many physical and chemical parameters influence chemical weathering rates, both in nature and in the laboratory. The following properties of aqueous fluids potentially influence the rates of dissolution for any particular mineral: temperature, pH, ionic strength, concentration of rate-enhancing catalysts or rate inhibitors, and fluid saturation state. Fluid saturation state is a thermodynamic measure of how far from equilibrium a particular dissolution (or precipitation) reaction occurs at. It is a unique rate-determining parameter because it provides a specific link between kinetics and thermodynamics.

Natural waters display varying degrees of saturation with respect to common rock-forming minerals, as reported in a comprehensive study by Stefánsson and Arnórsson (Stefánsson and Arnórsson, 2000). Their results show that at temperatures less than 50 °C, natural waters are in general undersaturated with respect to calcite, amorphous silica, albite (low and high), and anorthite, and close to saturation (or even over-saturated) with respect to chalcedony, quartz, microcline, and sanidine. At temperatures greater than 50 °C, natural waters are saturated with respect to all of these minerals, with the exception of anorthite, and amorphous silica. Variable degrees of fluid undersaturation and saturation with respect to feldspars and other major rock forming minerals have also been measured in pore fluids from soil profiles (White et al., 2001; White et al., 2002). Fluid–rock interactions have even been documented to occur to depths of several kilometers, based on deep drilling projects (Komninou and Yardley, 1997; Morrow et al., 1994; Project Management Programme, 1996; Rabemanana et al., 2003; Stober and Bucher, 1999), e.g., Soultz-sous-Fôrets, Rhine Graben, France, 5 km; KTB, Oberpfalz, Germany, 9 km; Kola Peninsula, Russia, 11 km. In these deep environments, with few exceptions, fluids are generally saturated or supersaturated with respect to most mineral phases.

Given that natural waters display a large range of fluid–mineral saturation states, in particular at low to moderate temperatures, it is important to understand the relation between mineral dissolution kinetics and fluid saturation state. At a microscopic level, the relation between dissolution rate and saturation state is intrinsically related to dynamic fluid–solid interface processes operating at a nano- to subnanometer scale. Thus, key aspects to the mechanism of dissolution can be derived from the rate-free energy relation. Studies relating rates with free energies can thus be considered to be complementary to direct nanoscale investigations of fluid–mineral reactions using such techniques as atomic force microscopy (AFM) (Drake and Hellmann, 1991; Hellmann et al., 1992) and transmission electron microscopy (TEM) (Hellmann et al., 2003; Hellmann et al., 2004). Moreover, at a macroscopic level, the temporal evolution of water–rock interactions is generally modeled using codes that incorporate rate laws that include a saturation state parameter. As will be shown in this study, the commonly used function that expresses the dependence of rate on saturation state may be inaccurate near equilibrium.

Despite the multi-scalar importance of free energy with respect to dissolution mechanisms and overall rate laws, only a limited number of theoretical (Aagaard and Helgeson, 1982; Bandstra and Brantley, 2008; Dove et al., 2005; Lasaga, 1981; Lasaga, 1995; Lasaga and Lüttge, 2004; Lüttge, 2006; Murphy and Helgeson, 1987) and experimental studies (Alekseyev et al., 1997; Beig and Lüttge, 2006; Berger, 1995; Berger et al., 2002; Brantley et al., 1986; Burch et al., 1993; Chen and Brantley, 1997; Gautier et al., 1994; Hellmann and Tisserand, 2006; Murakami et al., 1998; Nagy et al., 1991; Nagy and Lasaga, 1992; Oelkers, 2001; Taylor et al., 2000) have been devoted to unraveling this relation of fundamental importance. Here we report on recent results from two separate ongoing studies that are based on the dissolution kinetics of albite feldspar dissolution as a function of fluid saturation state. The feldspar family of minerals makes an ideal candidate for these types of studies because of the volumetric importance of feldspars in the upper crust (~75%, (Anderson, 1989)). The use of albite, the Na end-member of the feldspar plagioclase solid solution series, also has the advantage that it is perhaps the most thoroughly investigated feldspar phase with respect to published kinetic studies in the literature. The two complementary studies that we present here are based on an experimental determination of the dependence of dissolution rate (R) on fluid saturation state (ΔG_r) at two different conditions: basic pH at 150 °C ('study no. 1') and acid pH at 100 °C ('study no. 2'). The originality of this study is that we have investigated the same mineral at two very different pH and temperature regimes, thus allowing us to determine how these two parameters influence the R–ΔG_r relation for albite. The ultimate purpose of this comparison is to test whether there exists a universal R–ΔG_r behavior for a single mineral.

Aside from exploring questions of fundamental scientific importance in the second study (i.e., the R–ΔG_r relation at acid pH), the use of CO_2 as an acidifying medium to produce carbonic acid presents an additional interest associated with large-scale environmental applications, and in particular, understanding the consequences of massive CO_2 injection into geological repositories. It is well known that in the presence of aqueous solutions with high $f\,CO_2$, dissolution of Mg, Ca, and Fe silicates coupled to the reprecipitation of Mg, Ca, or Fe carbonates leads to a net consumption of CO_2 and its sequestration into a solid phase. Albite dissolution, at certain chemical conditions, can also lead to the precipitation of a solid phase, in this case dawsonite, $NaAlCO_3(OH)_2$ (Bénézeth et al., 2007; Hellevang et al., 2005; Knauss et al., 2005). In addition, geochemical models applied to CO_2 injection scenarios depend on the accurate prediction of rates of mineral dissolution (such as albite) and precipitation of secondary phases as a function of solution saturation state in order to model the evolution of porosity associated with the migration of a CO_2 plume in an underground aquifer or storage site (Le Guen et al., 2007).

2. Theory

A general formula for expressing the dissolution or precipitation of any feldspar is:

$$\mathrm{Na_xK_yCa_zAl_{1+z}Si_{3-z}O_8 + 8H_2O \rightarrow xNa^+ + yK^+ + zCa^{2+} + (1+z)Al(OH)_4^- + (3-z)H_4SiO_4^0} \quad (1)$$

where $x + y + z = 1$. The ion activity product of the above reaction can be expressed as:

$$Q = a_{Na^+}^{x} \cdot a_{K^+}^{y} \cdot a_{Ca^{2+}}^{z} \cdot a_{Al(OH)_4^-}^{(1+z)} \cdot a_{H_4SiO_4^0}^{3-z} \quad (2)$$

if the activities of the solid and water are taken to equal unity. If considering only pure albite, y and z equal zero in Eqs. (1) and (2). At chemical equilibrium, the ion activity product is equivalent to the equilibrium constant K. The saturation state of a fluid is often expressed in terms of the ratio (Q/K); if by common convention the dissolving mineral appears on the left side of the reaction, values of $(Q/K) < 1$ indicate undersaturation of the fluid with respect to the mineral, and conversely, $(Q/K) > 1$ is representative of supersaturation. In this study, however, we quantify the degree of undersaturation in terms of a thermodynamic parameter, the Gibbs free energy of reaction, ΔG_r. The Gibbs free energy is defined as:

$$\Delta G_r = RT\ln\left(\frac{Q}{K}\right) \quad (3)$$

where R is the gas constant ($J\,mol^{-1}\,K^{-1}$) and T is the temperature in Kelvin. At conditions of chemical equilibrium, $\Delta G_r = 0$, and as the degree of undersaturation increases, ΔG_r becomes increasingly negative.

The following general equation (adapted from (Lasaga, 1995); see also (Aagaard and Helgeson, 1982)) is often used to integrate rate-influencing parameters into an overall dissolution rate law for a given temperature:

$$R = k_+ a_{H^+,OH^-}^{n_{H^+},n_{OH^-}} g(I) \prod_i a_i^{n_i} f(\Delta G_r) \quad (4)$$

In the above rate law, the overall, surface area-normalized rate R (units of $mol\,m^{-2}\,s^{-1}$) is a function of the forward rate constant k_+ (units of $mol\,m^{-2}\,s^{-1}$), the activity a of either H^+ or OH^- raised to the corresponding exponential power n (note that if the reaction occurs in 'pure' water, the activity term refers to water and thus can be considered to equal unity), the ionic strength $g(I)$, the catalytic or inhibiting effect of certain aqueous species Πa, and the Gibbs free energy function $f(\Delta G_r)$. Very few studies have examined the effect of all of the above terms on mineral dissolution rates; in fact, the majority of mineral dissolution studies have determined rates only in terms of their pH and temperature dependence. Moreover, most experimental studies have been conducted at conditions far from equilibrium, where the $f(\Delta G_r)$ term is generally neglected under the assumption that $f(\Delta G_r) \approx 1$, which implies that the reaction rate is independent of the saturation state of the fluid. Because so few studies have addressed the influence of the $f(\Delta G_r)$ term, the driving force of our two studies was measuring the R–ΔG_r relation for albite feldspar, a common rock-forming mineral, and then determining if different conditions of dissolution change the nature of the dependence of dissolution rate on free energy.

3. Experiments

The results we report here are based on two separate studies of albite dissolution kinetics as a function of ΔG_r, the first at basic pH, the second at acid pH. Both of these studies are still in progress: study 1 is now in its 10th year, study 2 is in its 4th year. When dissolution reactions occur at conditions near equilibrium in flow through reactors, fluid residence times in the reactor can be very long (e.g. on the order of months), and mineral reaction rates are significantly slower than at far-from-equilibrium conditions. Because of these two reasons, we have paid particular attention to ensuring that each measured rate and corresponding ΔG_r is obtained at conditions representative of both hydrodynamic equilibrium (i.e., passage of at least 2–3 reactor volumes before measurement) and dynamic chemical equilibrium (i.e., steady-state concentrations in reactor over time intervals of several weeks at near equilibrium conditions). This reasoning explains the unusually long time periods associated with these experimental studies.

The experiments are run using flow through reactors based on a CSTR design (continuous stirred tank reactor; for reactor details, see ref. (Hellmann, 1999; Hellmann et al., 1997)). In all experiments, mm-sized albite grains are used that have been ultrasonically cleaned in alcohol. The specific surface area is measured by BET. The quantity of albite used for each experiment is such that only a monolayer of grains covers the floor of the reactor, thereby ensuring fluid circulation between the grains. The kinetics determined in each experiment always represent steady-state rates measured over time spans generally ranging from 1–2 weeks at far-from-equilibrium conditions, to month-long (and greater) periods closer to equilibrium. In

all cases, rates are measured after a minimum of three reactor volumes have passed through the reactor. Dissolution rates are continuously determined as a function of time and are based on the aqueous constituent elements collected at the output of the reactor, as well as mass loss; each rate reported from the first study represents the unweighted mean of three rates: $R_{\text{mass loss}}$, R_{Si} and R_{Al}; in the second study, only R_{Si} is used. The free energy of the dissolution reaction can be varied either by changing the solid to solution ratio, or by changing the residence time of the fluid in contact with the minerals. This is effected by changing the flow rate of the pump (decreasing the flow rate results in ΔG_r values closer to equilibrium).

In the first study, the dissolution of albite is measured at 150 °C, pH 9.2 (pH 10.0 25 °C), and 1.5 MPa fluid pressure. The input fluid is injected into the reactor (2 reactors used, 300 or 50 mL volume) with a HPLC pump. The input solution is a boric acid pH buffer (0.05 M H_3BO_3) that is adjusted to pH 10.0 (25 °C) using 1N NaOH. Because the Na concentration is fixed by the buffer ([Na] ≈ 0.039–0.043 m), only the concentrations of Al and Si vary with time and with free energy, and thus only these two elements are used to calculate the dissolution rate. However, the concentrations of all three elements (Na, Al, Si) are used to calculate free energies that correspond to discreet steady-state dissolution rates.

The second study is based on dissolution at acid pH conditions (i.e. high pCO_2) at 100 °C. These conditions were chosen since they are relevant for geological storage of CO_2 (Bachu, 2000). The experimental setup is based on two reactors connected in series. The first reactor is a 2 L autoclave that contains two separate phases: a denser phase of CO_2-saturated H_2O, and a less dense, supercritical CO_2 phase. During each experiment, pure H_2O is continuously pumped into the saturation autoclave where it contacts the supercritical CO_2. The contact (residence) time is sufficiently long to ensure the uptake and equilibration of CO_2 with the injected H_2O (residence times of 10^4–10^6 min, depending on flow rate). The CO_2-saturated water prepared at 25 °C is continuously injected into the main reactor (300 mL volume) where dissolution takes place at 100 °C. The pressure of the entire flow system, which includes the back pressure regulator, the main reactor, and the CO_2-saturation autoclave, is 9.0 MPa. This pressure corresponds to the partial pressure of CO_2 in the CO_2–H_2O solution. Using empirical correlation diagrams from Spycher et al. (Spycher et al., 2003) to determine the fugacity coefficient, the corresponding aqueous fugacity (f CO_2) and pH are 7.2 MPa and 3.25, respectively, as calculated by the geochemical code EQ3NR (Wolery, 1992). Because of assumed precipitation of Al as a discrete secondary phase during the experiment, only Si is used to calculate the rates of dissolution. However, the concentrations of all three elements (Na, Al, Si) are used to calculate free energies.

4. Results

The results we report on here are derived from two ongoing albite feldspar dissolution investigations. A large part of the data from the dissolution study at basic pH and 150 °C has been reported in a recent publication (Hellmann and Tisserand, 2006). Here we extend these results by comparing them with unpublished data from the second study that is based on dissolution at acid pH and 100 °C. This is the first publication that we know of that explicitly compares the R–ΔG_r relation for the same mineral at significantly different conditions of dissolution. As discussed in detail further on, even though the dissolution rates are different, both studies show dissolution rate-free energy relations (R–ΔG_r) that are very similar.

The data from the first study describe a sigmoidal relation between the rate R and the free energy ΔG_r, as shown in Fig. 1. The data are characterized by three distinct R–ΔG_r regions: a: far-from-equilibrium; b: transition; c: near-equilibrium. The data at far-from-equilibrium conditions, $\Delta G_r = -149$ to -70 kJ mol^{-1}, have a relatively high degree of dispersion, in large part attributable to analytical uncertainty associated with measurements at very low Si and Al concentration levels (10^{-7} m, ppb range). Because dissolution is most rapid at these conditions, each rate datum represents a separate experiment (note that only $\Delta G_r > -80$ kJ mol^{-1} data are represented in Fig. 1). This experimental protocol was used to avoid significant changes in surface area over time (i.e. pristine grains were used for each experiment run at a specific flow rate). A constant rate of approximately 1.0×10^{-8} mol m^{-2} s^{-1} describes the kinetic data in this free energy range. The constancy of the rates in this ΔG_r region represents an important kinetic phenomenon because the rates are independent of ΔG_r, and by definition, also independent of the concentrations of the aqueous dissolution products (in particular Si and Al). In this region, characterized by a 'rate plateau', rate laws can be written that do not include a free energy term (i.e. because $f(\Delta G_r) \approx 1$).

The second set of data lies nearer to equilibrium and extends from ~−70 to ~−25 kJ mol^{-1} (Fig. 1). In this free energy range, the dissolution rates are no longer constant, but rather abruptly decrease in a roughly linear manner with increasing ΔG_r; for this reason, this part of R–ΔG_r relation is called the 'transition' region. In this ΔG_r interval, the recorded rate closest to the upper ΔG_r bound is 3.1×10^{-9} mol m^{-2} s^{-1}, which was measured at a $\Delta G_r = -29.6$ kJ mol^{-1}. Thus, in the transition region the slowest recorded rate is only one third of the plateau rate. As was the case at far-from-equilibrium conditions, each datum point represents a separate experiment; however, the data are significantly less dispersed. Overall, dissolution is stoichiometric in the transition region, as well as at far from equilibrium. The sudden decrease in the dissolution rate in the transition region is not due to pH, as the pH remained constant in the reactor based on EQ3NR calculations. Moreover, the effect of secondary precipitates on the rates can also be excluded.

The third set of data represents near-equilibrium conditions, and is delimited by free energies that extend from ~−25 to 0 kJ mol^{-1}, where the latter value represents chemical equilibrium. At the lower bound of this region (~−25 kJ mol^{-1}), the slope of the R–ΔG_r relation becomes much shallower, and is characterized by a much weaker, inverse dependence of the rate on free energy. The recorded rates that were measured are clustered with respect to ΔG_r

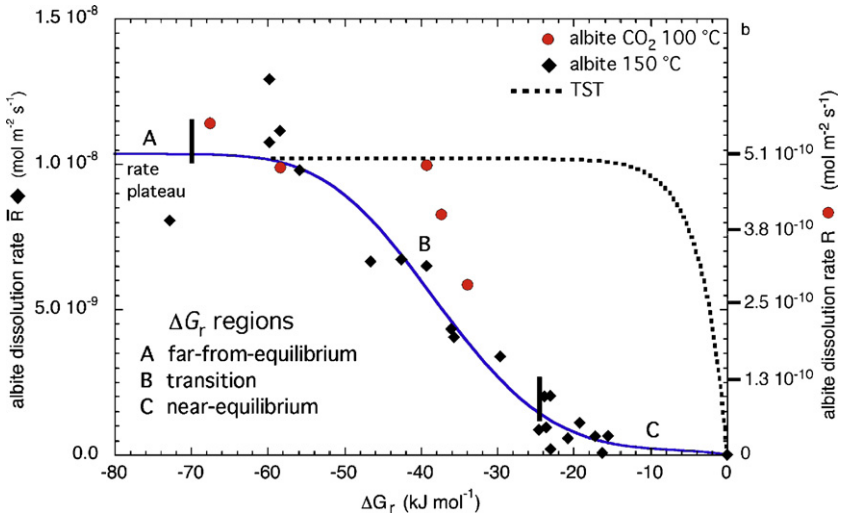

Fig. 1. Dissolution rates (R) of albite measured as a function of the Gibbs free energy (ΔG_r) at acid pH (filled circles) and basic pH (filled diamonds). The data and the fitted rate curve (Eq. (5) in text) define three R–ΔG_r regions: far-from-equilibrium (which coincides with a rate plateau), transition, and near-equilibrium. The dashed line represents a rate curve using a TST-based free energy parameter.

Fig. 1. Vitesse de dissolution (R) de l'albite en fonction de l'enthalpie libre de la réaction (ΔG_r) à pH acide (cercles pleins) et basique (losanges pleins). Les données et la courbe ajustée suivant l'équation 5 (cf. texte) décrivent trois domaines différents : une zone loin de l'équilibre, où la relation R–ΔG_r décrit un plateau, une zone de transition et une zone proche de l'équilibre. La ligne en pointillés représente une courbe paramétrée suivant le formalisme de la théorie de l'état de transition (TST).

between −24.6 and −15.6 kJ mol^{-1}. The minimum recorded rate in this region, 6.2×10^{-11} mol m^{-2} s^{-1}, is slightly more than two orders of magnitude lower than the plateau rate, 1.0×10^{-8} mol m^{-2} s^{-1}. In the near-equilibrium region, five separate experiments were used to generate the rates that are plotted in Fig. 1; however, because these rates were by far slower than those at conditions further from equilibrium (i.e., transition, plateau rate regions), each separate experiment yielded up to four different and separate R–ΔG_r data points. This was achieved by varying the flow rate. This experimental protocol required that each rate measurement be acquired at steady-state conditions. Because dissolution at near-equilibrium conditions occurs much more slowly, this necessitated single experiments that were run over periods of up to several hundred days in order to ensure steady-state rate conditions at each flow rate (e.g., the longest single experiment ran for 641 d). In order to measure rates even closer to equilibrium, current experiments are being run at $\Delta G_r > -15$ kJ mol^{-1}.

Results from the second investigation are based on dissolution at acid pH and 100 °C. At present, we can only report on five R–ΔG_r data that were obtained from one single experiment that has been in continuous operation for almost 600 d. Nonetheless, despite the still limited nature of this data set, the overall shape of the data points to a non-linear, sigmoidal R–ΔG_r relation. The three rates representative of conditions furthest from equilibrium, obtained at ΔG_r between −68 and −39 kJ mol^{-1}, represent a dissolution rate plateau, where the average rate is 5.1×10^{-10} mol m^{-2} s^{-1}. The two other rates (4.1×10^{-10}, 2.8×10^{-10} mol m^{-2} s^{-1}), obtained, respectively, at $\Delta G_r = -37$ and −34 kJ mol^{-1}, define the transition region since they mark a sharp decrease in the dissolution rate compared to the plateau rate. These preliminary results are plotted in Fig. 1 (note the use of different rate scales for both studies).

The results at acid pH can be examined with respect to several points. The plateau rate of 5.1×10^{-11} mol m^{-2} s^{-1} ($\log R = -9.3$) can be compared to an extrapolated rate of 1.2×10^{-9} mol m^{-2} s^{-1} ($\log R = -8.9$) at pH 3.25, 100 °C, based on the dissolution of albite using HCl/H_2O solutions (see results in (Hellmann, 1994; Hellmann, 1995)). Given the scatter in the rates in both studies, the two rates are very comparable. However, the uncertainty in the rates makes it difficult, if not impossible, to determine whether an intrinsic kinetic effect can be attributed to the presence of aqueous CO_2 at high concentrations. A second point of importance concerns the abrupt decrease in rates (Fig. 1) that occurs over a range in free energies between −39 and −37 kJ mol^{-1}. This notable decrease in rates is real and cannot be attributed to an increase in pH. Albeit the weak buffering capacity of the CO_2–H_2O solution, the pH of the solution in the reactor did not increase by more than 0.2 pH units, based on calculations using EQ3NR. At $\Delta G_r > -40$ kJ mol^{-1}, the stoichiometry of the dissolution process became increasingly incongruent, based on the measured elemental release rates ($R_{Si} \approx R_{Na} \gg R_{Al}$). The precipitation of a secondary Al-bearing phase(s) (e.g. Al -[oxi]hydroxide) is the most likely reason, which is supported by EQ3NR-derived mineral saturation indices calculated from the aqueous chemistries of samples. In addition, past experience with albite dissolution at elevated temperatures and at acid pH conditions reveals that secondary Al-bearing phases, such as boehmite, predominate (Hellmann, 1999; Hellmann et al., 1989), but because of their high porosity, they do not appear to have an effect on the rate of dissolution.

5. Discussion

The continuous and highly non-linear, sigmoidal relation between the dissolution rate R and the free energy ΔG_r described by the data from the first study, and partially from the second study, can be fit with any number of mathematical relations. We have chosen the approach of Burch et al. (Burch et al., 1993) and fit the data (first study only) to a rate law that is based on the sum of two parallel rate processes:

$$R = k_1[1 - \exp(-ng^{m1})] + k_2[1 - \exp(-g)]^{m2}. \quad (5)$$

where k_1 and k_2 are rate constants that have been determined by regression, with values 1.02×10^{-8} and 1.80×10^{-10} mol m^{-2} s^{-1}, $g \equiv |\Delta G_r|/RT$ is a dimensionless number, and n, m_1, and m_2 are adjustable fitted parameters ($n = 7.98 \times 10^{-5}$, $m_1 = 3.81$ and $m_2 = 1.17$). The overall rate based on the fitted rate curve can be seen in Fig. 1. Fig. 2 is a close up view showing the kinetic data at near-equilibrium conditions, as well as the fitted overall rate curve that represents the sum of two separate, parallel rate processes. For two rate processes occurring in parallel, the faster one determines the overall rate.

The parallel rate law developed by Burch and co-workers (Burch et al., 1993) that was applied to their experimental data for albite dissolution at basic pH and 80 °C has both experimental and theoretical underpinnings. According to these authors, the use of a parallel rate law implies that, "dissolution proceeds simultaneously at each 'site' on the surface and at a rate governed by the energetics of the local surface environment and the bulk solution undersaturation, ΔG_r". These authors made the observation that extensive etch pit formation only occurred at high undersaturations, whereas at near-equilibrium conditions, most of the grains appeared unaltered, with a very low density of etch pits that were small and shallow. This observation, in conjunction with an abrupt change in rate with decreasing free energy at approximately -30 kJ mol^{-1}, led them to suggest that a major change in dissolution mechanism occurs between the near-equilibrium and far-from-equilibrium regions. They quantified this by proposing that when the free energy of the dissolution reaction is below a certain critical value, extensive etch pit development occurs, i.e., $\Delta G_r < \Delta G_r^{\text{crit}}$ (equivalent to high degrees of undersaturation), and conversely, when $\Delta G_r > \Delta G_r^{\text{crit}}$, etch formation is not favored, and dissolution occurs at other sites, such as cleavage steps and grain edges. It is interesting to note that the existence of a critical free energy ('critical supersaturation') and an associated change in mechanism was originally postulated in a theoretical study of crystal growth by Burton, Cabrera and Frank (Burton et al., 1951); for additional details on how BCF theory has been applied to dissolution, see refs. (Lasaga and Blum, 1986; Lasaga and Lüttge, 2001; Lasaga and Lüttge, 2004).

Referring back to Fig. 2, the two parallel rate processes that comprise the overall rate law (Eq. (5)) are denoted by curves B and C. At near-equilibrium conditions, rate process C predominates, whereas at conditions far from equilibrium process B predominates. The intersection of the two curves, at -15 kJ mol^{-1}, represents the free energy where there is a switch in the predominant mechanism of dissolution, and hence is equivalent to ΔG_r^{crit}. However, the scatter in the experimental data set (Fig. 2) suggests that the value of ΔG_r^{crit} cannot be exactly determined, but rather

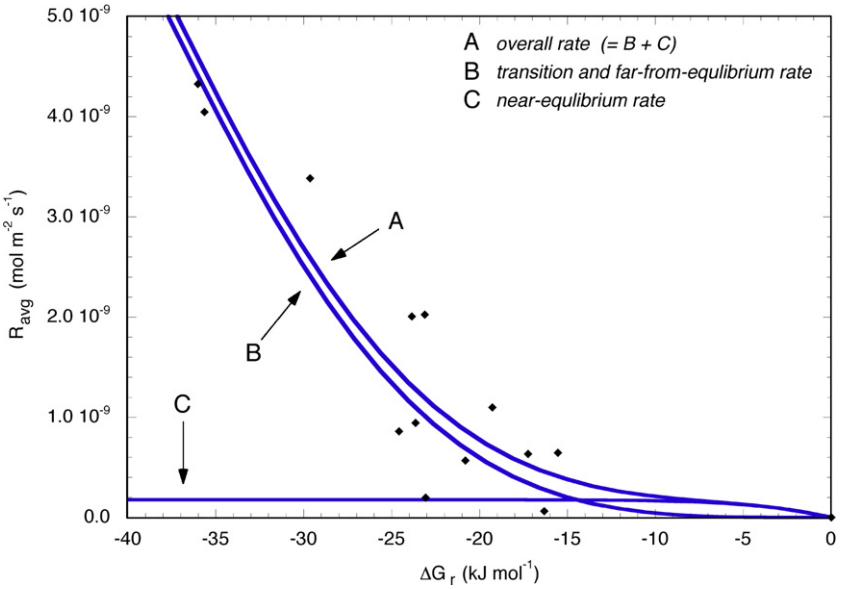

Fig. 2. Close up of transition and near-equilibrium R–ΔG_r regions. The black diamonds are the measured rates, and A represents the overall fitted rate curve, which is based on the sum of two independent and parallel rates, denoted by B and C.

Fig. 2. Vue détaillée de la fin de la zone de transition et de la zone à proximité de l'équilibre chimique. Les losanges noirs correspondent aux vitesses mesurées et A représente la courbe d'ajustement sur le jeu complet de données. Cette courbe est construite à partir de la somme de deux vitesses indépendantes et parallèles représentées par les courbes B et C.

should be assigned to a range in free energies extending from −15 to −25 kJ mol^{-1}. It is interesting to note that the microtopography of the grains reflects the influence of ΔG_r, as evidenced by well-developed, geometric etch pits and angular edges formed at $\Delta G_r < \Delta G_r^{crit}$, and irregular pitting and rounded edges at conditions $\Delta G_r > \Delta G_r^{crit}$. Fig. 3a,b amply show the difference in grain morphology, at the millimeter scale, between two samples that underwent dissolution at $\Delta G_r = -17$ and -25 kJ mol^{-1}, respectively (see also Figs. 6 and 7 in ref. (Hellmann and Tisserand, 2006)). This example is important in that it readily illustrates how a small difference in free energy (8 kJ mol^{-1}) can shift surface reactions from one predominant mechanism to another when dissolution occurs in the vicinity of ΔG_r^{crit}.

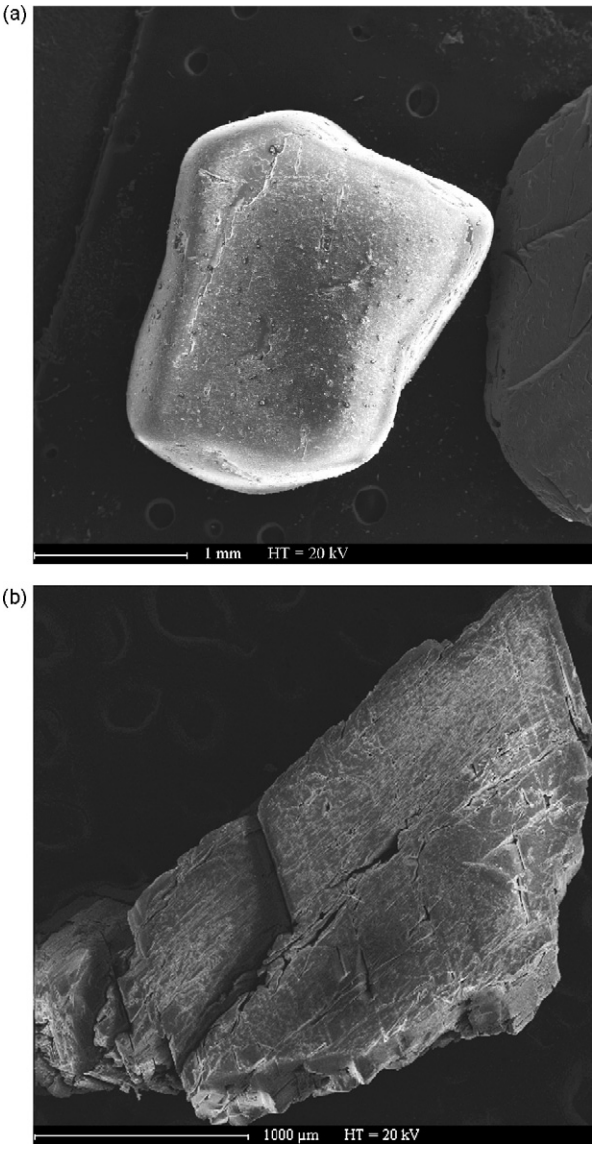

Fig. 3. Morphology of grains after dissolution, as a function of solution saturation state. a: experiment 50 N, 227 d, $\Delta G_{r\ final} = -17$ kJ mol^{-1}; b: experiment 300 S, 641 d, $\Delta G_{r\ final} = -25$ kJ mol^{-1} (for details concerning these experiments, see ref. (Hellmann and Tisserand, 2006)).

Fig. 3. Morphologie des grains après dissolution, en fonction de l'état de saturation en fin d'expérience. a : expérience 50 N, 227 jours, $\Delta G_{r\ finale} = -17$ kJ mol^{-1} ; b : expérience 300 S, 641 jours, $\Delta G_{r\ finale} = -25$ kJ mol^{-1} (pour des détails concernant les expériences, voir réf. (Hellmann and Tisserand, 2006)).

At a fundamental, mechanistic level, one of the most important results from our two studies is the similar nature of the dissolution rate dependence on free energy; in both cases the relation is a highly non-linear, sigmoidal function, despite differences in the conditions of dissolution (i.e., basic vs. acid pH, 150 vs. 100 °C, respectively). The rate-retarding effect of aqueous Al is often cited by Oelkers and co-workers (Oelkers et al., 1994; Oelkers, 2001) as being one of the principal kinetic factors causing the decrease in the overall rate with increasing solution saturation. It is therefore interesting to note that the evolution of bulk Al concentrations as a function of increasing solution saturation is quite different in our two studies. At basic pH conditions [Al] increases continuously with increasing solution saturation, whereas at acid pH, [Al] concentrations decrease significantly over the same free energy range ($\Delta G_r > -40$ kJ mol^{-1}) where the rates begin to decrease sharply. Thus, despite the differences in the behavior of [Al] with increasing ΔG_r, the measured R–ΔG_r relations are very similar. This observation is at odds with the role of Al proposed by Oelkers et al. (Oelkers et al., 1994; Oelkers, 2001). Moreover, in the aforementioned study by Burch et al. (Burch et al., 1993), the authors show by way of isokinetic diagrams that the decrease in rates with approach to chemical equilibrium cannot be attributed to individual mechanisms of rate inhibition by either aqueous Si or Al.

The non-linear, sigmoidal behavior of the R–ΔG_r relations measured in our two studies, coupled to the observation that the sharp decreases in rates occur within a free energy interval of ∼10 kJ mol^{-1} of each other, leads to the question as to whether this represents some kind of universal behavior (i.e. pH and temperature independent) behavior for albite, and perhaps other feldspars, as well. The aforementioned study by Burch et al. (Burch et al., 1993) also shows a R–ΔG_r relation for albite that is non-linear and sigmoidal, with a ΔG_r^{crit} of ∼−30 kJ mol^{-1}, which compares favorably with our estimate of −15 to −25 kJ mol^{-1} at basic pH conditions. Moreover, published studies in the literature of other feldspar phases, such as K-feldspar, sanidine, and labradorite, carried out at different pH and temperature conditions, are in accord with a non-linear, sigmoidal dependence of dissolution rate on free energy (Alekseyev et al., 1997; Beig and Lüttge, 2006; Berger et al., 2002; Taylor et al., 2000). This perhaps lends support to the idea of a certain universal behavior describing the dependence of the dissolution rate on the free energy with respect to all of the feldspars. Nonetheless, some studies show R–ΔG_r data for feldspars that do not show this non-linear, sigmoidal behavior (Gautier et al., 1994; Oelkers, 2001). Nonetheless, an in-depth analysis of the discrepancies between the various feldspar studies is beyond the scope of this publication.

If a non-linear, sigmoidal relation between dissolution rate and free energy is, arguably, the most accurate general description for the kinetic behavior of feldspars as a function of solution saturation state, many important

questions remain. One of these concerns the nature of the transition region, and in particular, the influence of both the aqueous environment (pH, temperature, ionic strength, presence of inhibitors or catalysts) and the solid phase on the value of ΔG_r^{crit}. This has obvious consequences with respect to the mechanism of dissolution as a function of solution saturation state. Another point of importance is the continuity of the R–ΔG_r relation. In our first experimental study (and partially with respect to the second study), the experimental data show good continuity, extending from conditions at far from equilibrium, traversing the transition region, and continuing at near-equilibrium conditions. In nearly all studies (ours and most other published studies), the experimental protocol is such that to achieve measurements at near-equilibrium conditions, fluids in contact with the solids evolve towards higher solution saturations (i.e., increasing ΔG_r), and thus the measured dissolution rates (in transition and near-equilibrium regions) may be influenced by etch pits and other surface topography features that form during the initial stages of dissolution at conditions far from equilibrium. Lüttge and co-workers have argued that the R–ΔG_r relation is dependent on the reaction history of the solid phase (Beig and Lüttge, 2006; Lüttge, 2006), such that different rates (for the same mineral) are theoretically possible at an identical ΔG_r, depending on whether the particular ΔG_r value is approached from lower or higher free energies. In fact, Lüttge (Lüttge, 2006) makes the case that any rate data falling in the steep transition region represent non-steady state phenomena, and can be attributed to experimental protocol (i.e., initiation of experiments at far-from-equilibrium conditions). To summarize, Lüttge (Lüttge, 2006) proposes that mineral systems dissolve at near-equilibrium conditions with one mechanism (curve C in Fig. 2), and at ΔG_r^{crit}, the dissolution rate jumps to the plateau rate in a discontinuous manner (i.e., in this case, the transition region is not sigmoidal, but rather a step function jump), and remains at the plateau rate for all $\Delta G_r \leq \Delta G_r^{crit}$. Thus, for dissolution conditions where $\Delta G_r \leq \Delta G_r^{crit}$ holds, the rate mechanism is the sum of the near-equilibrium rate and the plateau rate. This controversy points out that more experimental work needs to be done in order to verify or disprove this idea.

One last, but very important point needs to be made concerning the mathematical form of the free energy parameter, $f(\Delta G_r)$. In our two studies, the data and the fitted rate curve are non-linear and sigmoidal. However, by far the vast majority of geochemical codes used to model non-equilibrium water–rock interactions use kinetic rate laws that incorporate a $f(\Delta G_r)$ parameter that is loosely based on 'transition state theory' (TST). So-called TST-based free energy terms have the following general form (Aagaard and Helgeson, 1982; Lasaga, 1981):

$$f(\Delta G_r) = \left[1 - \exp\left(n\frac{\Delta G_r}{RT}\right)\right] \quad (6)$$

where n is an exponent related to the nature of the activated complex ($n = 1$ corresponds to a dissolution mechanism controlled by the breakdown of a single activated complex; (Lasaga et al., 1994; Lasaga, 1998). Fig. 1 shows the rate data from our two studies, the fitted rate curve based on Eq. (5), and a rate curve using the TST free energy parameter given by Eq. (6) ($n = 1$) and a plateau rate with $k_+ = 1.02 \times 10^{-8}$ mol m^{-2} s^{1}). Aside from predicting a R–ΔG_r relation that is completely at odds with the sigmoidal relation we propose, the TST rate curve significantly overestimates the dissolution rate at near-equilibrium conditions, by up to an order of magnitude. This may be particularly important when water–rock interactions are modeled at elevated temperatures where near-equilibrium rates are easily attained. A second shortcoming of the TST rate curve is that it predicts rates independent of ΔG_r at far too high levels of solution saturation. While the data in our studies are still restricted in scope, they nonetheless point out the utility of further investigations into the dependence of dissolution rates on free energy with respect to other important rock-forming minerals, and in particular, with respect to improving the accuracy of geochemical codes used to model non-equilibrium water–rock interactions.

Acknowledgements

The first dissolution study was primarily funded by the following programs: Arc géothermie du PIRSEM, Arc géothermie des roches fracturées, DBT II-INSU "Fluides dans la croûte", ECODEV, EC contract ENK5-2000-00301 (years 2001-2004), EGS Pilot Plant EC contract SES-CT-2003-502706 (years 2005-2008). The second study has been funded by Gaz de France (contract no. 722478/00; program coordinators C. Rigollet, S. Saysset, and R. Dreux; contract managed by F. Renard at LGIT, Grenoble). The SEM images shown in Fig. 3 were taken by S. Pairis, Institut Néel, Grenoble. We also acknowledge the help of D. Faivre (ENS-Lyon) during his 1998 summer internship in our laboratory.

References

Aagaard, P., Helgeson, H.C., 1982. Thermodynamic and kinetic constraints on reaction rates among minerals and aqueous solutions. I. Theoretical considerations. Am. J. Sci. 282, 237–285.

Alekseyev, V.A., Medvedeva, L.S., Prisyagina, N.I., Meshalkin, S.S., Balabin, A.I., 1997. Change in the dissolution rates of alkali feldspars as a result of secondary mineral precipitation and approach to equilibrium. Geochim. Cosmochim. Acta 61, 1125–1142.

Anderson, D.L., 1989. Theory of the Earth. Blackwell Scientific Publications, Oxford, UK, 366 p.

Bachu, S., 2000. Sequestration of CO_2 in geological media: criteria and approach for site selection in response to climate change. Energy Convers. Mgmt. 41, 953–970.

Bandstra, J.Z., Brantley, S.L., 2008. Surface evolution of dissolving minerals investigated with a kinetic Ising model. Geochim. Cosmochim. Acta 72, 2587–2600.

Beig, M.S., Lüttge, A., 2006. Albite dissolution kinetics as a function of distance from equilibrium: Implications for natural feldspar weathering. Geochim. Cosmochim. Acta 70, 1402–1420.

Bénézeth, P., Palmer, D.A., Anovitz, L.M., Horita, J., 2007. Dawsonite synthesis and reevaluation of its thermodynamic properties from solubility measurements: Implications for mineral trapping of CO_2. Geochim. Cosmochim. Acta 71, 4438–4455.

Berger, G., 1995. The dissolution rate of sanidine between 100 and 300 °C, In: Y.K. Kharaka, O. Chudaev (Eds.), Water-Rock Interaction WRI-8, Balkema, Rotterdam, NL, 141–144.

Berger, G., Beaufort, D., Lacharpagne, J.-C., 2002. Experimental dissolution of sanidine under hydrothermal conditions: Mechanism and rate. Am. J. Sci. 302, 663–685.

Brantley, S.L., Crane, S.R., Crerar, D.A., Hellmann, R., Stallard, R., 1986. Dissolution at dislocation etch pits in quartz. Geochim. Cosmochim. Acta 50, 2349–2361.

Burch, T.E., Nagy, K.L., Lasaga, A.C., 1993. Free energy dependence of albite dissolution kinetics at 80 °C and pH 8.8. Chem. Geol. 105, 137–162.

Burton, W.K., Cabrera, N., Frank, F.C, 1951. The growth of crystals and their equilibrium structure of their surfaces, Royal Soc. London Phil. Trans. 243 (ser. A) 299–358.

Chen, Y., Brantley, S.L., 1997. Temperature and pH-dependence of albite dissolution rate at acid pH. Chem. Geol. 135, 275–290.

Dove, P.M., Han, N., De Yoreo, J.J., 2005. Mechanisms of classical crystal growth theory explain quartz and silicate dissolution behavior. Proc. Natl. Acad. Sci. 43, 15357–15362.

Drake, B., Hellmann, R., 1991. Atomic force microscopy imaging of the albite (010) surface. Am. Mineral. 76, 1773–1776.

Gautier, J.-M., Oelkers, E.H., Schott, J., 1994. Experimental study of K-feldspar dissolution rates as a function of chemical affinity at 150 °C and pH 9. Geochim. Cosmochim. Acta 58, 4549–4560.

Hellevang, H., Aagaard, P., Oelkers, E.H., Kvamme, B., 2005. Can dawsonite permanently trap CO_2? Environ. Sci. Technol. 39, 8281–8287.

Hellmann, R., 1994. The albite-water system: Part I. The kinetics of dissolution as a function of pH at 100, 200 and 300 °C. Geochim. Cosmochim. Acta 58, 595–611.

Hellmann, R., 1995. The albite-water system Part II. The time-evolution of the stoichiometry of dissolution as a function of pH at 100, 200 and 300 °C. Geochim. Cosmochim. Acta 59, 1669–1697.

Hellmann, R., 1999. The dissolution behavior of albite feldspar at elevated temperatures and pressures: the role of surface charge and speciation. Mitteil. Österr. Mineral. Gesell. 144, 13–44.

Hellmann, R., Tisserand, D., 2006. Dissolution kinetics as a function of the Gibbs free energy of reaction: An experimental study based on albite feldspar. Geochim. Cosmochim. Acta 70, 364–383.

Hellmann, R., Crerar, D.A., Zhang, R., 1989. Albite feldspar hydrolysis to 300 °C. Solid State Ionics 32/33, 314–329.

Hellmann, R., Drake, B., Kjoller, K., 1992. Using atomic force microscopy to study the structure, topography and dissolution of albite surfaces. In: Kharaka, Y.K., Maest, A.S. (Eds.), Water-Rock Interaction 7, I. A.A. Balkema, Rotterdam, pp. 149–152.

Hellmann, R., Dran, J.-C., Della Mea, G., 1997. The albite-water system Part III. Characterization of leached and hydrogen-enriched layers formed at 300 °C using MeV ion beam techniques. Geochim. Cosmochim. Acta 61, 1575–1594.

Hellmann, R., Penisson, J.-M., Hervig, R.L., Thomassin, J.-H., Abrioux, M.-F., 2003. An EFTEM/HRTEM high-resolution study of the near surface of labradorite feldspar altered at acid pH: evidence for interfacial dissolution-reprecipitation. Phys. Chem. Minerals 30, 192–197.

Hellmann, R., Penisson, J.-M., Hervig, R.L., Thomassin, J.-H., Abrioux, M.-F., 2004. Chemical alteration of feldspar: a comparative study using SIMS and HRTEM/EFTEM. In: Wanty, R.B., Seal, II, R.R. (Eds.), Water Rock Interaction. A.A. Balkema, Rotterdam, NL, pp. 753–756.

Knauss, K.G., Johnson, J.W., Steefel, C.I., 2005. Evaluation of the impact of CO_2, co-contaminant gas, aqueous fluid and reservoir rock interactions on the geologic sequestration of CO_2. Chem. Geol. 217, 339–350.

Komninou, A., Yardley, B.W.D., 1997. Fluid-rock interactions in the Rhine Graben: A thermodynamic model of the hydrothermal alteration observed in deep drilling. Geochim. Cosmochim. Acta 61, 515–531.

Lasaga, A.C, 1981. Transition state theory, In: A.C. Lasaga, R.J. Kirkpatrick (Eds.), Kinetics of Geochemical Processes, Vol. 8, pp. 135–169. Mineralogical Society of America, Washington, D.C., USA, pp. 135–169.

Lasaga, A.C., 1995. Fundamental approaches in describing mineral dissolution and precipitation rates. In: White, A.F., Brantley, S.L. (Eds.), Chemical Weathering Rates of Silicate Minerals, 31. Mineralogical Society of America, Washington, D.C., USA, pp. 23–86.

Lasaga, A.C., 1998. Kinetic Theory in the Earth Sciences. Princeton University Press, Princeton, USA, 811 p.

Lasaga, A.C., Blum, A.E., 1986. Surface chemistry, etch pits and mineral-water interactions. Geochim. Cosmochim. Acta 50, 2363–2379.

Lasaga, A.C., Lüttge, A., 2001. Variation of crystal dissolution rate based on a dissolution stepwave model. Science 291, 2400–2404.

Lasaga, A.C., Lüttge, A., 2004. Mineralogical approaches to fundamental crystal dissolution kinetics. Amer. Mineral. 89, 527–540.

Lasaga, A.C., Soler, J.M., Ganor, J., Burch, T.E., Nagy, K.L., 1994. Chemical weathering rate laws and global geochemical cycles. Geochim. Cosmochim. Acta 58, 2361–2386.

Le Guen, Y., Renard, F., Hellmann, R., Brosse, E., Collombet, M., Tisserand, D., Gratier, J.-P., 2007. Enhanced deformation of limestone and sandstone in the presence of high pCO_2 fluids. J. Geophys. Res. 112, B05421, doi:10.1029/2006JB004637.

Lüttge, A., 2006. Crystal dissolution kinetics and Gibbs free energy. J. Electron Spectrosc. Relat. Phenom. 150, 248–259.

Morrow, C., Lockner, D., Hickman, S., Rusanov, M., Röckel, T., 1994. Effects of lithology and depth on the permeability of core samples from the Kola and KTB drill holes. J. Geophys. Res. 99, 7263–7274.

Murakami, T., Kogure, T., Kadohara, H., Ohnuki, T., 1998. Formation of secondary minerals and its effect on anorthite dissolution. Am. Mineral. 83, 1209–1219.

Murphy, W.H., Helgeson, H.C., 1987. Thermodynamic and kinetic constraints on reaction rates among minerals and aqueous solutions. III. Activated complexes and the pH-dependence of the rates of feldspar, pyroxene, wollastonite, and olivine hydrolysis. Geochim. Cosmochim. Acta 51, 3137–3153.

Nagy, K.L., Lasaga, A.C., 1992. Dissolution and precipitation kinetics of gibbsite at 80 °C and pH 3: the dependence on solution saturation state. Geochim. Cosmochim. Acta 56, 3093–3111.

Nagy, K.L., Blum, A.E., Lasaga, A.C., 1991. Dissolution and precipitation kinetics of kaolinite at 80 °C and pH 3: the dependence on solution saturation state. Am. J. Sci. 291, 649–686.

Oelkers, E.H., 2001. General kinetic description of multioxide silicate mineral and glass dissolution. Geochim. Cosmochim. Acta 65, 3703–3719.

Oelkers, E.H., Schott, J., Devidal, J.-L., 1994. The effect of aluminum, pH, and chemical affinity on the rates of aluminosilicate dissolution rates. Geochim. Cosmochim. Acta 58, 2011–2024.

Project Management of the Continental Deep Drilling Programme of the FRG in the Geol. Survey of Lower Saxony, KTB, Report 95-2 KTB Hauptbohrung. Results of Geoscientific Investigation in the KTB Field Laboratory. Final report: 0-9191 m, E. Schweizerbart'sche, Stuttgart, Germany, 1996, 228 p.

Rabemanana, V., Durst, P., Bächler, D., Vuataz, F.-D., Kohl, T., 2003. Geochemical modelling of the Soultz-sous-Forêts Hot Fractured Rock system. Comparison of two reservoirs at 3.8 and 5 km depth. Geothermics 32, 645–653.

Spycher, N., Pruess, K., Ennis-King, J., 2003. CO_2-H_2O mixtures in the geological sequestration of CO_2. I. Assessment and calculation of mutual solubilities from 12 to 100 °C and up to 600 bar. Geochim. Cosmochim. Acta 67, 3015–3031.

Stefánsson, A., Arnórsson, S., 2000. Feldspar saturation state in natural waters. Geochim. Cosmochim. Acta 64, 2567–2584.

Stober, I., Bucher, K., 1999. Deep groundwater in the crystalline basement of the Black Forest region. Appl. Geochem. 14, 237–254.

Taylor, A.S., Blum, J.D., Lasaga, A.C., 2000. The dependence of labradorite dissolution and Sr isotope release rates on solution saturation state. Geochim. Cosmochim. Acta 64, 2389–2400.

White, A.F., Bullen, T.D., Schulz, M.S., Blum, A.E., Huntington, T.G., Peters, N.E., 2001. Differential rates of feldspar weathering in granitic regoliths. Geochim. Cosmochim. Acta 65, 847–869.

White, A.F., Blum, A.E., Schulz, M.S., Huntington, T.G., Peters, N.E., Stonestrom, D.A., 2002. Chemical weathering of the Panola Granite: Solute and regolith elemental fluxes and the weathering rate of biotite. In: Hellmann, R., Wood, S.A. (Eds.), Water-Rock Interactions, Ore Deposits, and Environmental Geochemistry A Tribute to David A. Crerar, 7. The Geochemical Society, St. Louis, USA, pp. 37–59.

Wolery, T.J, 1992. EQ3NR, A Computer Program for Geochemical Aqueous Speciation-Solubility Calculations: Theoretical Manual, User's Guide, and Related Documentation (Version 7.0). Lawrence Livermore Natl. Lab. UCRL-MA-110662 PT III., USA, 246 p.